6420 *J. Phys. Chem. A* **1999,** *103,* 6420−6428

Vibrational Assignment and Dipole Moment Derivatives of Liquid Bromobenzene at 25 °C

C. Dale Keefe,* Leslie A. Donovan, and Stephen D. Fleet

Department of Physical and Applied Sciences, University College of Cape Breton,
Sydney, Nova Scotia, Canada B1P 6L2

Received: March 15, 1999; In Final Form: June 5, 1999

The previously published optical constants of bromobenzene were used to calculate the imaginary molar polarizability spectrum. The imaginary molar polarizability spectrum was fit to 163 classical damped harmonic oscillator bands between 3240 and 140 cm^{-1}, the vast majority of which were obvious in the experimental spectrum. With the aid of the previous fundamental assignments in the literature and the force field for liquid benzene, the first thorough assignment of liquid bromobenzene is presented. The integrated intensities, transition moments, and dipole moment derivatives with respect to normal coordinates of the fundamentals were calculated from the fitted bands. These transition moments and dipole moment derivatives are compared with those in the literature for benzene-*d*. The transition moments and dipole moment derivatives are significantly different in these substituted benzenes, indicating that either the eigenvectors for the vibrations are different in the two molecules or that dipole moment derivatives with respect to internal coordinates are different in the two molecules. This will be analyzed further in a future paper.

Introduction

In a previous paper from this laboratory[1] the optical constants (real and imaginary refractive indices) of bromobenzene were reported across the mid-infrared. In this paper, these results are combined with far-infrared measurements in the literature[2] to give the optical constants between 3240 and 28 cm^{-1}. From these optical constants, the chemically more important imaginary molar polarizability spectrum, $\alpha_m''(\tilde{\nu})$, was calculated under the Lorentz local field, using equations described in the literature.[3] The complete optical constant, dielectric constant, and imaginary polarizability spectra are available at http://faculty.uccb.ns.cal∼dkeefe/spectra.

The imaginary molar polarizability spectrum was fitted between 3240 and 140 cm^{-1} to separate the integrated intensities due to different transitions. Most of the required peaks were due to observable features within the spectrum. The assignment of most of the features in the infrared spectrum of liquid bromobenzene is reported for the first time.

Experimental

Imaginary Refractive Indices. In a previous paper[1] from this laboratory, the optical constants of liquid bromobenzene were reported between 3240 and 421 cm^{-1}. These optical constants were measured using standard experimental techniques described in the literature.[4−6] In the previous paper, the dipole moment derivatives with respect to normal coordinates of the infrared active fundamentals above 421 cm^{-1} were calculated by a simple numeric integration over a given wavenumber region. This technique could not separate the contributions of overlapping bands, nor could it guarantee the complete integrated intensity even for well-separated bands. To achieve this, it is necessary to fit the spectra.

The previous measurements did not include the fundamentals below 421 cm^{-1}; accordingly, the region below 421 cm^{-1} was taken from the literature. The portion of the spectrum between 361 and 28 cm^{-1} was obtained by scanning the far-infrared linear napierian absorption coefficient spectrum of liquid bromobenzene given by Fleming et al.[2] The scanned far IR

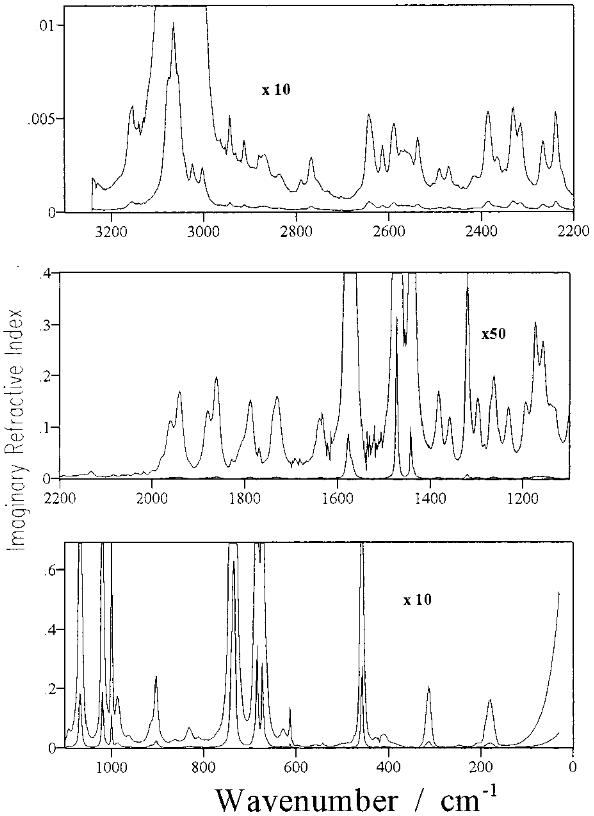

Figure 1. Imaginary refractive index spectrum, $k(\tilde{\nu})$, of liquid C_6H_5-Br at 25 °C between 3240 and 28.4 cm^{-1}. The upper spectrum in the top and bottom boxes shows the experimental spectrum multiplied by 10. The upper spectrum in the middle box shows the experimental spectrum multiplied by 50.

---

* To whom correspondence should be addressed. Fax: 902-562-0119. E-mail: dkeefe@uccb.ns.ca.

10.1021/jp990902q CCC: $18.00

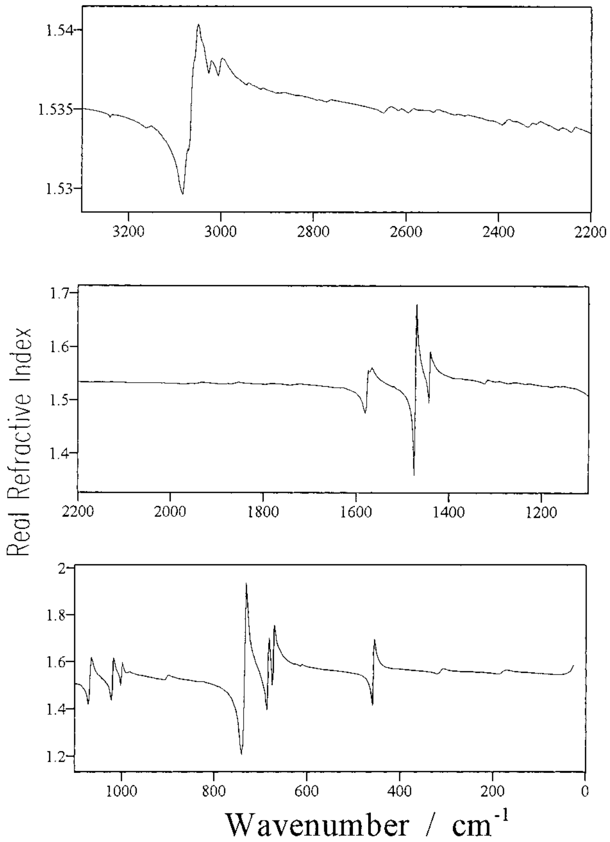

Figure 2. Real refractive index spectrum, $n(\tilde{\nu})$, of liquid C_6H_5Br at 25 °C between 3240 and 28.4 cm^{-1}.

spectrum was manually digitized, using Paintshop Pro, at 206 points. These data were smoothed with a three point moving average. The digitized data were plotted on the same scale as the original publication, and the two overlaid. There was no significant variation between the two. The resulting data were converted to imaginary refractive indices via

$$k(\tilde{\nu}) = \alpha(\tilde{\nu})/(4\pi\tilde{\nu}) \qquad (1)$$

where $\alpha(\tilde{\nu})$ is the linear napierian absorption coefficient, not to be confused with $\alpha''_m(\tilde{\nu})$ used below for the imaginary molar polarizability. To obtain the 0.4821168 cm^{-1} spacing of the previous measurements from this laboratory, the imaginary refractive indices were linearly interpolated between the digitized points. Fleming et al.[2] do not comment on the accuracy or precision of their measurements and thus the accuracy of the imaginary refractive indices below 361 cm^{-1} is not known.

This interpolated spectrum was merged with the previously reported imaginary refractive index spectrum, with the region between 421 and 361 cm^{-1} linearly interpolated. The imaginary refractive indices between 421 and 361 cm^{-1} are extremely weak and no values could be obtained from the graphs given by Jones.[5] The resulting imaginary refractive index spectrum is shown in Figure 1.

Real Refractive Indices. The real refractive indices were calculated from the above imaginary refractive indices by Kramers–Kronig transformation with $n_{8000} = 1.5372 \pm 0.0003$.[1] This value of n_{8000} was obtained by fitting the literature[7] real refractive indices at four visible wavelengths and extrapolating to 8000 cm^{-1}. To improve the accuracy of the calculated real refractive indices, the values of k between 8000 and 3240 cm^{-1} were assumed to be 0 and values of k were linearly extrapolated from 0.0528 at 28.4 cm^{-1} to 0 at 0 cm^{-1}.[8] The estimated uncertainty of the real refractive indices depends on the uncertainty of the value of n_{8000}, the uncertainty of the numerical Kramers–Kronig transformation,[8] and the uncertainty of the imaginary refractive indices. The uncertainty of the real refractive indices between 3200 and 421 cm^{-1} is estimated to be ~0.2%.[1,9–12] The accuracy of the imaginary refractive indices below 421 cm^{-1} is not known. A 10% uncertainty in the imaginary refractive indices will contribute a 10% uncertainty in the value of $\Delta n(\tilde{\nu}) = n(\tilde{\nu}) - n_{8000}$, which corresponds to ~0.05–0.25% uncertainty in $n(\tilde{\nu})$ below 421 cm^{-1}. Thus, it is reasonable to assume that the $n(\tilde{\nu})$ values below 421 cm^{-1} have an uncertainty of 0.2–0.5%. The real refractive index spectrum is shown in Figure 2.

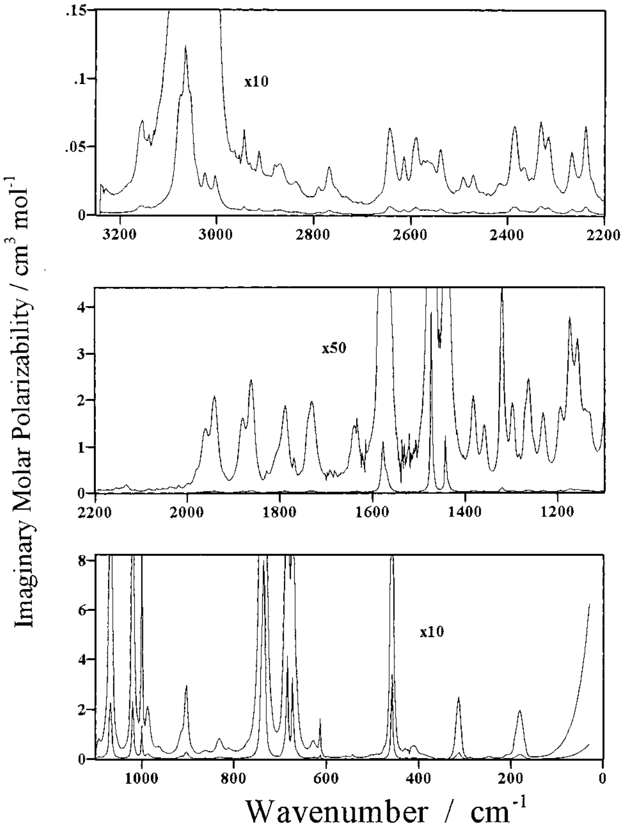

Figure 3. Imaginary molar polarizability spectrum, $\alpha''_m(\tilde{\nu})$, of liquid C_6H_5Br at 25 °C between 3240 and 28.4 cm^{-1}. The upper spectrum in the top and bottom boxes shows the experimental spectrum multiplied by 10. The upper spectrum in the middle box shows the experimental spectrum multiplied by 50.

Molar Polarizability Spectra. The real and imaginary molar polarizability spectra were calculated from the complex refractive index spectra by program DEQUANT[13] using the molar volume of 105.51 mL/mol.[1] The imaginary molar polarizability spectrum is shown in Figure 3.

Fitting the Imaginary Molar Polarizability Spectrum. The imaginary molar polarizability spectrum between 3240 and 140 cm^{-1} was fitted with classical damped harmonic oscillator (CDHO) bands[3] using the curve-fitting program YACFIT5.[13] This program requires the user to input the peak parameter file and the spectrum to be fitted. In addition, the user has the option to input a parameter file containing fixed peaks and/or a baseline. To hasten the fitting process, the bromobenzene spectrum was split into three regions. Each of these regions was then fitted separately until a satisfactory fit was obtained. When fitting the narrower wavenumber regions, it was sometimes necessary to include a linear baseline to account for the wings of the intense and/or broad peaks outside the region.

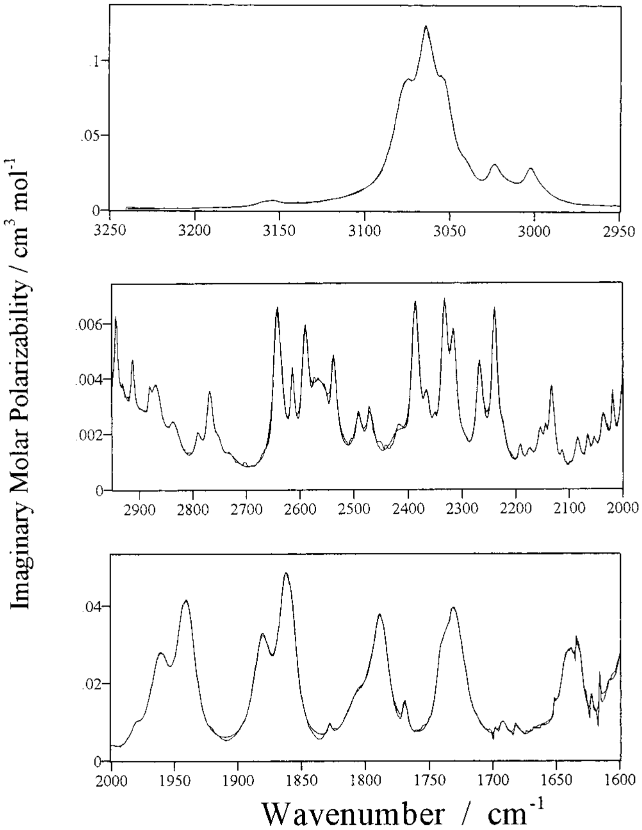

Figure 4. The experimental and fitted imaginary molar polarizability spectra of liquid C_6H_5Br at 25 °C between 3240 and 1600 cm^{-1}.

After the narrower wavenumber regions were fitted, the peak parameters for each region were merged together (baselines that were included in the narrower wavenumber regions were not included) and then input into YACFIT5 along with the full bromobenzene spectrum and the parameters refined. The fit required 163 peaks. In most cases, the bands were needed to fit obvious peaks, shoulders, or asymmetry in the experimental spectrum; in a small number of cases, the bands are simply there to improve the fit, indicating that some peaks may not have a CDHO line shape. The standard deviation of the fit is 1.1×10^{-2}, the root-mean-square error is 1.0×10^{-2}, and the multiple coefficient of determination,[14] R^2, is 0.9995, indicating a near perfect fit. An important check, for our purposes, is the agreement of the total areas under both the experimental and fitted spectra. The total area under the fitted spectrum between 3240 and 140 cm^{-1} is 0.5% larger than the total area under the experimental spectrum.

The parameters obtained from YACFIT5 are $\tilde{\nu}_j$, the peak wavenumber; Γ_j, the full width at half height; and a constant Y_j, that is the peak height of the corresponding band in the $\tilde{\nu}\alpha''_m$ spectrum.[13] The complete integrated intensity under the $\tilde{\nu}\alpha''_m$ band, C_j, can be obtained from Y_j by $C_j = Y_j\pi/2$. The parameters $\tilde{\nu}_j$, Γ_j, and C_j of the fitted bands are tabulated in Table 1. It is estimated that the C_j values obtained in this way are accurate to about 10%.[13]

The quality of the fit is shown in Figures 4 and 5, which contain both the experimental and fitted spectra. In the top box of Figure 4, there is no visible difference between the two spectra. In the middle box, noticeable differences occur at ~2800, ~2700, ~2450, and ~2415 cm^{-1}, where the fitted spectrum is lower than the experimental, and at ~2550 cm^{-1}, where the fitted spectrum is higher. In the lower box, noticeable differences occur at ~1910 and ~1840 cm^{-1}, where the fitted spectrum is higher, and at ~1750 and ~1615 cm^{-1}, where the fitted spectrum is lower.

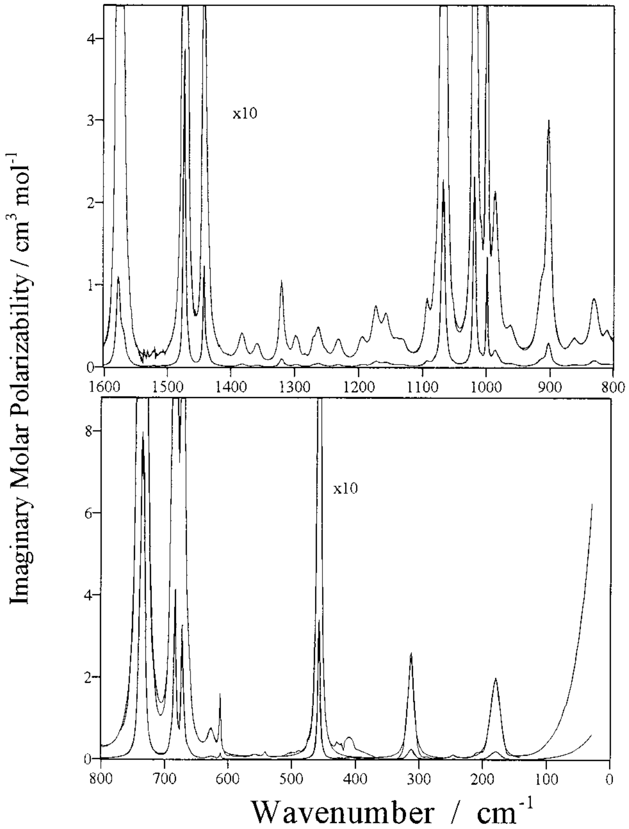

Figure 5. The experimental and fitted imaginary molar polarizability spectra of liquid C_6H_5Br at 25 °C between 1600 and 140 cm^{-1}. The upper spectra in each box are the experimental and fitted spectra multiplied by 10.

In Figure 5, the fitted and experimental spectra are shown both on the ordinate scale given in the figure as well as multiplied by ten. On the true scale, there is no visible difference between the fitted and experimental spectra. On the expanded scale, the only noticeable differences are at ~1040, ~700, ~335, ~290, and ~155 cm^{-1}, where the fitted spectrum is higher, and at ~205 cm^{-1}, where the fitted spectrum is lower.

The quality of the fit and the peaks used to fit the experimental spectrum are illustrated in Figures 6−8. Shown in these figures are the experimental and fitted imaginary molar polarizability spectra for three regions of varying intensity, 3240 to 2950 cm^{-1} (weak), 2000 to 1700 cm^{-1} (very weak), and 1100 to 950 cm^{-1} (strong). In the upper boxes, both the experimental and fitted spectra are given. The only visible differences are in Figure 7 at ~1910, ~1840, and ~1775 cm^{-1}, where the fitted spectrum is higher, and at ~1750 and ~1705 cm^{-1}, where the fitted spectrum is lower. The peaks used to calculate the fitted spectrum in each region are shown in the bottom boxes. It should be noted that the wings of all the peaks outside the region are included in the fitted spectrum, but for clarity these are not shown. Fourteen peaks are required to fit the region 3240 to 2950 cm^{-1} and 17 peaks are required to fit the region 2000 to 1700 cm^{-1}, all visible in the experimental spectrum as peaks, shoulders, or changes of slope. Thirteen peaks are required to fit the region 1100 to 950 cm^{-1}, with all but the peaks at 1069.5, 1020.7, and 993.6 cm^{-1} obvious in the experimental spectrum.

Discussion

Assignment of Transitions. The vibrational representation for monohalobenzenes is $11A_1 + 3A_2 + 6B_1 + 10B_2$ under the

TABLE 1: Observed and Fitted Bands in the Imaginary Molar Polarizability Spectrum of Liquid Bromobenzene

		fitted band			
assignment[a]	obsd $\tilde{\nu}$[b]	$\tilde{\nu}_j$[c]	Γ_j[c]	C_j[d]	sum of C_j[d]
$2\nu_4$ (A_1) (3157)	3159 sh vw	3159.9	8.1	79.7	
$\nu_4+\nu_{23}$ (B_2) (3148)	3153.3 vw	3153.4	10.0	130.0	
	tail	3096.9	117.6	2498.8	7483.9
ν_{21} (B_2)	3075.0 w	3076.9	16.3	4985.1	
ν_1 (A_1)	3064.5 m	3064.4	11.4	4568.7	
$3\nu_8$ (A_1) (3058)	3062 sh w	3059.8	4.7	143.1	
ν_2 (A_1)	3054 sh w	3053.4	12.8	3488.3	
ν_3 (A_1)	3041 sh w	3040.3	10.8	534.5	
ν_{22} (B_2)	3023.9 w	3023.8	8.4	672.0	
$\nu_{23}+\nu_{24}$ (A_1) (3012); $\nu_4+\nu_{24}$ (B_2) (3021)	tail	3016.7	16.6	564.0	
	3002.6, w	3002.6	7.0	398.7	
$3\nu_9$ (A_1) (2999)	tail	2999.6	21.5	1157.3	
	~2975 vw	I			
$3\nu_{15}$ (B_1) (2960)	2962.3 vw	2961.8	21.6	124.4	
$2\nu_5$ (A_1) (2948)	2952.4 vw	2952.6	1.8	5.2	
	2946.5 vw	I			
$4\nu_{17}$ (A_1) (2945)	2942.9 vw	2942.8	7.2	107.3	
	2930.4 vw	2929.7	22.9	141.0	
$\nu_5+\nu_{24}$ (B_2) (2917)	~2922 vw	I			
	2912.1 vw	2912.0	7.9	79.4	
	~2902 vw	I			
$\nu_4+\nu_{25}$ (B_2) (2899)	~2895 vw	2897.7	32.2	160.3	
$\nu_{23}+\nu_{25}$(B_1) (2891); $\nu_{21}-\nu_{20}$ (B_2) (2892)	~2890 vw	I			
$2\nu_{24}$ (A_1) (2885); $\nu_1-\nu_{20}$ (B_1) (2880)	2879.9 vw	2880.1	5.7	21.8	
$\nu_2-\nu_{20}$ (B_1) (2869)	2869.0 vw	2868.3	25.8	281.2	
$\nu_{23}+\nu_{26}$ (A_1) (2833)	2836.6 vw	2834.7	29.0	171.0	
$\nu_5+\nu_{25}$ (B_2) (2795)	2789.6 vw	2790.0	15.2	67.6	
$\nu_{24}+\nu_{25}$ (A_1) (2764); $\nu_{21}-\nu_{11}$(B_2) (2764)	2767.9 vw	2767.9	14.3	163.6	
$\nu_4+\nu_6$ (A_1) (2752) $\nu_1-\nu_{11}$ (A_1) (2752)	2755 sh vw	2752.2	15.7	46.3	
$\nu_{23}+\nu_{27}$ (A_1) (2727); $\nu_4+\nu_{27}$ (B_2) (2736) $\nu_5+\nu_{26}$ (B_2) (2738)	2735 vw	2730.5	37.0	87.2	
$2\nu_{25}$ (A_1) (2642); $\nu_4+\nu_7$ (A_1) (2646); $\nu_5+\nu_6$ (A_1) (2648); $\nu_4+\nu_{28}$ (B_2) (2648); $\nu_{23}+\nu_{28}$ (A_1) (2639)	2643.4 vw	2641.8	18.6	445.1	
$\nu_6+\nu_{24}$ (B_2) (2616); $\nu_{22}-\nu_{14}$ (B_1) (2615)	2614.3 vw	2614.2	7.9	80.7	
$\nu_{24}+\nu_{27}$ (A_1) (2600); $\nu_2-\nu_{19}$ (B_1) (2596); $\nu_4+\nu_8$ (A_1) (2598)	2595 sh vw	I			
$\nu_{25}+\nu_{26}$ (A_1) (2584); $\nu_8+\nu_{23}$ (B_2) (2589)	2589.4 vw	2590.5	13.4	199.3	
$\nu_4+\nu_9$ (A_1) (2578)	~2575 vw				
$\nu_4+\nu_{15}$ (B_1) (2565)$\nu_9+\nu_{23}$ (B_2) (2569)	~2566 vw				
	~2555 vw	2564.3	55.0	706.1	
$\nu_5+\nu_7$ (A_1) (2541); $\nu_5+\nu_{28}$ (B_2) (2544)	2538.4 vw	2537.0	11.2	120.2	
$\nu_7+\nu_{24}$ (B_2) (2510)	2504 vw	I			
$\nu_5+\nu_8$ (A_1) (2493); $\nu_6+\nu_{25}$ (B_2) (2495)	2491.9 vw	2492.4	18.4	109.2	
$\nu_5+\nu_9$ (A_1) (2474)	2470.8 vw	2470.0	19.8	134.4	
ν_1-ν_{29} (B_2) (2452)	2452 vw	I			
$\nu_9+\nu_{24}$ (B_2) (2442); ν_2-ν_{29} (B_2) (2441); $\nu_6+\nu_{26}$ (B_2) (2437)	2440 vw	I			
$\nu_{26}+\nu_{27}$ (A_1) (2421); ν_{22}-ν_{29} (A_1) (2411)	2415.9 wv	2419.7	43.7	202.1	
$\nu_7+\nu_{25}$ (B_2) (2388)	2385.8 vw	2385.8	17.0	362.8	
$\nu_5+\nu_{16}$ (B_1) (2377); $\nu_2-\nu_{18}$ (B_1) (2370); $\nu_3-\nu_{10}$ (A_1) (2368)	2366.2vw	2364.8	13.6	90.3	
$2\nu_6$ (A_1) (2347); $\nu_{22}-\nu_{10}$ (B_2) (2352)	2350.6 vw	2351.3	9.5	21.2	
$\nu_{26}+\nu_{28}$ (A_1) (2333); $\nu_7+\nu_{26}$ (B_2) (2331); $\nu_6+\nu_{27}$ (B_2) (2331)	2331.0 vw	2331.8	16.0	315.3	
$2\nu_{27}$ (A_1) (2315); $\nu_4+\nu_{17}$ (B_1) (2314); ν_2-ν_{17} (B_1) (2317)	2315.8 vw	2314.9	14.9	219.8	
	2296 sh vw	2296.1	16.6	29.1	
$\nu_9+\nu_{26}$ (B_2) (2263); $\nu_4+\nu_{18}$ (B_1) (2262)	2266.9 vw	2266.5	16.6	215.6	
$\nu_6+\nu_7$ (A_1) (2241); $\nu_6+\nu_{28}$ (B_2) (2243) $\nu_{10}+\nu_{23}$ (B_2) (2242)	2238.8 vw	2238.8	12.9	248.7	
$\nu_{27}+\nu_{28}$ (A_1) (2227); $\nu_{12}+\nu_{26}$ (B_1) (2225); $\nu_7 +\nu_{27}$ (A_1) (2225)	2224 br sh vw	2223.0	20.5	64.7	
$\nu_4+\nu_{29}$ (B_2) (2191); $\nu_6+\nu_8$ (A_1) (2193); ν_{22}-ν_{13} (B_1) (2191)	2191.7 vw	2191.5	10.0	26.2	
$\nu_6+\nu_9$ (A_1) (2173); $\nu_8+\nu_{27}$ (B_2) (2177)	2174.2 vw	2174.0	15.4	35.5	
$\nu_{13}+\nu_{25}$ (B_1) (2154); $\nu_9+\nu_{27}$ (B_2) (2157); $\nu_6 +\nu_{15}$ (B_1) (2160); $\nu_5+\nu_{18}$ (B_1) (2158)	2154.1 vw	2154.5	13.1	58.0	
$\nu_5+\nu_{10}$ (A_1) (2146); $2\nu_{28}$ (A_1) (2139)	2144.1 vw	2144.2	6.8	20.0	
$2\nu_7$ (A_1) (2135); $\nu_7+\nu_{28}$ (B_2) (2137)	2133.0 vw	2133.2	10.2	90.8	
$\nu_{18}+\nu_{24}$ (A_2) (2127)	2132 sh vw	2127.9	9.0	19.1	
$\nu_{10}+\nu_{24}$ (B_2) (2115); $\nu_{12}+\nu_{27}$ (B_1) (2119); ν_{21}-ν_{12} (B_1) (2115)	2113.7 vw	2113.3	7.0	11.3	
$\nu_5+\nu_{29}$ (B_2) (2087); $\nu_8+\nu_{28}$ (B_2) (2089); $\nu_7+\nu_8$ (A_1) (2087); $\nu_5+\nu_{29}$(B_2) (2087)	2084.1 vw	2084.4	11.7	39.8	
$\nu_7+\nu_9$ (A_1) (2067); ν_1-ν_9 (A_1) (2065); $\nu_9+\nu_{28}$ (B_2) (2069); ν_2-ν_{15} (B_1) (2067)	2065.9 vw	2065.5	7.4	21.8	
$\nu_7+\nu_{15}$ (B_1) (2054); $\nu_{24}+\nu_{29}$ (A_1) (2055)	2053.7 vw	2053.7	8.3	17.2	
$\nu_4+\nu_{19}$ (B_1) (2036); $\nu_{12}+\nu_{28}$ (B_1) (2031); $2\nu_8$ (A_1) (2038)	2036.8 vw	2036.0	13.6	64.3	
$\nu_8+\nu_9$ (A_1) (2019)	2018.7 vw	2018.6	5.2	28.4	
$2\nu_9$ (A_1) (1999); $\nu_1-\nu_7$ (A_1) (1997)	1999.2 vw	2000.1	7.1	31.0	
$\nu_{14}+\nu_{23}$ (B_1) (1979)	1979 sh vw	1981.1	9.2	100.7	
	1961.2 w	1961.9	18.9	1319.3	
$\nu_{12}+\nu_{15}$ (B_2) (1948)	1943 sh w	1944.2	13.1	774.3	
$\nu_{10}+\nu_{26}$ (B_2) (1935)	1940.9 w	1938.3	13.7	978.6	

TABLE 1: (Continued)

		fitted band			
assignment[a]	obsd $\tilde{\nu}^{b}$	$\tilde{\nu}_j^{c}$	Γ_j^{c}	C_j^{d}	sum of C_j^{d}
$\nu_{11}+\nu_{23}$ (B_2) (1882)	1880.5 w	1881.3	16.2	1260.6	
$\nu_{12}+\nu_{16}$ (B_2) (1864)	1861.9 w	1863.6	12.6	1224.0	
$\nu_{6}+\nu_{18}$ (B_1) (1858)	tail	1857.7	10.4	582.2	
$\nu_{6}+\nu_{10}$ (A_1) (1846)	1843.5 vw	I			
$\nu_{10}+\nu_{27}$ (B_2) (1829)	1828.4 vw	1828.2	3.3	29.4	
$\nu_{4}+\nu_{30}$ (B_2) (1825)	1824.1 vw	I			
$2\nu_{16}$ (A_1) (1805); $\nu_{7}+\nu_{17}$ (B_1) (1803)	1806 br sh w	1806.6	21.7	639.0	
$\nu_{5}+\nu_{11}$ (A_1) (1787); $\nu_{6}+\nu_{29}$ (B_2) (1786); $\nu_{2}-\nu_{26}$ (B_2) (1790)	1789.0 w	1788.7	16.3	1511.0	
$\nu_{27}+\nu_{29}$ (A_1) (1770)	1769.6 w	1769.0	3.9	75.5	
$\nu_{10}+\nu_{28}$ (B_2) (1742); $\nu_{1}-\nu_{25}$ (B_2) (1743)	1741 sh w	1740.8	10.3	484.3	
$\nu_{9}+\nu_{17}$ (B_1) (1736); $\nu_{13}+\nu_{16}$ (B_2) (1735); $\nu_{7}+\nu_{10}$ (A_1) (1739)	1736 sh w	1736.5	5.5	57.3	
$\nu_{14}+\nu_{25}$ (B_1) (1730); $\nu_{2}-\nu_{25}$ (B_2) (1732)	1731.8 w	1731.4	11.8	761.7	
$\nu_{5}+\nu_{30}$ (B_2) (1721); $\nu_{15}+\nu_{17}$ (A_1) (1723)	Tail, w	1725.1	13.9	562.8	
	Tail, w	1711.9	18.1	128.4	
wv	vw	1698.3	1.1	5.0	
$\nu_{24}+\nu_{30}$ (A_1) (1689); $\nu_{8}+\nu_{10}$ (A_1) (1691)	1692.5 w	1692.3	8.1	110.2	
$\nu_{28}+\nu_{29}$ (A_1) (1682); $\nu_{7}+\nu_{29}$ (B_2) (1680); $\nu_{9}+\nu_{18}$ (B_1) (1684)	1682.0 vw	1681.2	7.3	70.8	
$2\nu_{13}$ (A_1) (1666)	~1660 br sh vw	1664.6	18.6	177.2	
wv	1651.4 w	1651.3	2.8	26.4	
$\nu_{12}+\nu_{18}$ (B_2) (1646) $\nu_{16}+\nu_{17}$ (A_1) (1638)	1643.3 sh w	1642.5	12.0	585.8	
wv	1639.2 w	1638.4	3.3	33.5	
$\nu_{6}+\nu_{19}$ (B_1) (1631); $\nu_{11}+\nu_{25}$ (B_1) (1634); $\nu_{8}+\nu_{29}$ (B_2) (1632); ν_{21}-ν_{24} (A_1) (1634)	1633.0 sh w	1632.9	8.2	400.9	
wv	1622.3 w	1622.3	1.4	17.2	
wv	1615.9 w	1615.8	0.9	25.7	
$\nu_{9}+\nu_{29}$ (B_2) (1612); $\nu_{2}-\nu_{24}$ (B_2) (1610)		1609.0	6.2	77.5	
$\nu_{16}+\nu_{18}$ (A_1) (1586); $\nu_{22}+\nu_{24}$ (A_1) (1582)		1582.1	6.2	1726.3	
ν_{4} (A_1)	1578.1 s	1578.4	5.5	12954.4	
wv	1576.1 sh m	1576.0	1.8	845.8	
$\nu_{12}+\nu_{29}$ (B_1) (1574); $\nu_{11}+\nu_{26}$ (B_2) (1756); $\nu_{10}+\nu_{16}$ (B_1) (1574)	1571 sh m	1573.4	5.0	1768.9	
ν_{23} (B_2)	1570 sh m	1569.6	7.8	5844.4	
$\nu_{14}+\nu_{27}$ (B_1) (1566)	1562 sh m	1562.2	5.9	401.4	
wv	1557 w	1557.0	1.2	39.3	
wv	1553 w	I			
wv	1549 w	I			
wv	1543 w	I			
wv	1541 w	I			
wv	1537 w	I			
wv	1532 w	1531.6	1.5	30.1	
wv	1521 w	1522.8	4.0	81.7	
wv	1520 w	1520.3	0.005	900.9	
wv	1517 w	I			
wv	1512 w	I			
$\nu_{26}+\nu_{30}$ (A_1) (1510)	1510 w	1510.8	7.3	76.4	
wv	1506	I			
wv	1505	I			
vw	1498	I			
wv	1495	I			
$\nu_{1}-\nu_{23}$ (B_2) (1495)	1490 sh w	1491.4	17.5	182.8	
$\nu_{6}+\nu_{11}$ (A_1) (1486); $\nu_{1}-\nu_{4}$ (A_1) (1486)	1486 sh w	I			
$\nu_{14}+\nu_{28}$ (B_1) (1479); $\nu_{8}+\nu_{19}$ (B_1) (1477); $\nu_{2}-\nu_{4}$ (A_1) (1475)		1475.7	1.0	894.5	
ν_{5} (A_1)	1473.9 s	1474.1	3.0	25811.0	
$2\nu_{17}$ (A_1) (1472)		1472.2	1.9	2611.8	
$\nu_{11}+\nu_{27}$ (B_2) (1470); $\nu_{3}-\nu_{23}$ (B_2) (1471)	1468 sh m	1468.4	5.5	2683.1	
$\nu_{9}+\nu_{19}$ (B_1) (1457); $\nu_{22}-\nu_{23}$ (A_1) (1454)	1456	I			
$\nu_{13}+\nu_{29}$ (B_1) (1445); $\nu_{15}+\nu_{19}$ (A_1) (1444); $\nu_{22}-\nu_{4}$ (B_2) (1445)		1443.6	2.3	2314.2	11284.7
ν_{24} (B_2)	1442.9 s	1442.6	3.0	5825.0	
	1438 br sh m	1437.8	7.9	2937.1	
	tail w	1426.5	11.1	208.4	
$\nu_{12}+\nu_{19}$ (B_2) (1419); $\nu_{6}+\nu_{30}$ (B_2) (1420); $\nu_{17}+\nu_{18}$ (A_1) (1420)	1418.7 w	1418.0	8.7	101.3	
$\nu_{27}+\nu_{30}$(A_2) (1404); $\nu_{10}+\nu_{17}$ (B_1) (1408)	1404.3 w	1406.6	13.4	96.6	
$\nu_{11}+\nu_{28}$ (B_2) (1382); $\nu_{7}+\nu_{11}$ (A_1) (1380)	1383.0 w	1383.0	13.7	1061.8	
$\nu_{6}+\nu_{20}$ (B_1) (1358); $\nu_{16}+\nu_{19}$ (A_1) (1360)	1359.4 w	1361.1	9.3	293.2	
$\nu_{10}+\nu_{18}$ (B_1) (1356)	tail w	1356.7	8.6	220.0	
ν_{25} (B_2)	1321.0 m	1321.0	7.6	1540.9	
$\nu_{9}+\nu_{11}$ (A_1) (1312); $\nu_{28}+\nu_{30}$ (A_1) (1316); $\nu_{14}+\nu_{16}$ (B_2) (1311); $\nu_{7}+\nu_{30}$ (B_2) (1314)	1313 sh w	1312.9	9.2	140.3	
$\nu_{11}+\nu_{5}$ (B_1) (1299)	1298.6 w	1299.7	9.1	443.5	
$\nu_{13}+\nu_{19}$ (B_2) (1290)	1296 sh w	1295.2	7.5	227.2	
$\nu_{10}+\nu_{29}$ (B_2) (1284)	1284.2 w	1284.3	4.4	38.5	
	1271 sh w	1271.8	6.0	180.4	1283.0
ν_{26}(B_2)	1263.9 w	1263.4	13.2	1102.6	

TABLE 1: (Continued)

		fitted band			
assignment^a	obsd $\tilde{\nu}^b$	$\tilde{\nu}_j^c$	Γ_j^c	C_j^d	C_j^d
$\nu_7+\nu_{20}$ (B_1) (1252); $\nu_{23}-\nu_{11}$ (B_2) (1257)	1253 sh w	1251.6	7.1	66.4	
$\nu_5-\nu_{30}$ (B_2) (1228)	1232.0 w	1232.1	14.5	787.9	
$\nu_{17}+\nu_{19}$ (A_1) (1194); $\nu_{24}-\nu_{30}$ (A_1) (1196)	1194.7 w	1195.1	13.9	677.0	
ν_6 (A_1)	1173.5 w	1173.6	13.7	1502.2	
ν_{27} (B_2)	1157.4 w	1157.3	14.6	1308.9	
$\nu_{12}+\nu_{20}$ (B_2) (1146)	tail w	1149.3	5.1	14.9	
$\nu_{18}+\nu_{19}$ (A_1) (1142)	1141.5 w	1141.9	11.9	252.1	
	1136 sh w	1135.3	10.9	199.0	
$\nu_{10}+\nu_{19}$ (B_1) (1130); $\nu_{24}-\nu_{11}$ (B_2) (1130)	1131.3 w	1129.1	10.7	272.9	
$\nu_{14}+\nu_{18}$ (B_2) (1093)	1093.6 w	1093.6	8.5	755.8	
$\nu_{13}+\nu_{30}$ (B_1) (1079)	tail m	1081.2	5.3	198.4	
ν_{28} (B_2)		1069.5	4.5	9774.8	
ν_7 (A_1)	1068.4 s	1067.2	5.3	12711.3	
$\nu_{11}+\nu_{17}$ (B_1) (1049)	1052.4 w	I			
$\nu_{14}+\nu_{29}$ (B_1) (1021)		1020.7	3.3	2346.0	
ν_8 (A_1)	1019.1 s	1019.1	3.7	11813.2	
$\nu_{13}+\nu_{20}$ (B_2) (1017); $\nu_{26}-\nu_{30}$ (A_1) (1017) $\nu_5-\nu_{19}$ (B_1) (1017)	tail m	1015.5	6.0	1368.4	
$\nu_{25}-\nu_{11}$ (B_2) (1008)	1009 sh m	1008.4	4.5	322.3	
ν_9 (A_1)	999.4 s	999.6	2.4	4850.1	
$\nu_{11}+\nu_{18}$ (B_1) (997); $\nu_6-\nu_{20}$ (B_1) (989)	tail m	993.6	142.7	10.7	
ν_{15} (B_1)	986.7 m	986.7	10.4	2750.4	
$\nu_{10}+\nu_{11}$ (A_1) (985)	982 br sh m	981.6	9.2	459.8	
ν_{12} (A_2)	961.2 w	961.6	18.1	840.9	
$2\nu_{19}$ (A_1) (915); $\nu_{10}+\nu_{30}$ (B_2) (918) $\nu_{25}-\nu_{14}$ (B_1) (912)	913 br sh m	914.9	13.6	1237.4	
ν_{16} (B_1)	902.6 m	902.4	8.9	3509.5	
$\nu_4-\nu_{18}$ (B_2) (895)	891 sh w	I			
$\nu_{29}+\nu_{30}$ (A_1) (859); $\nu_5-\nu_{29}$ (B_2) (862); $\nu_6-\nu_{11}$ (A_1) (861); $\nu_{10}+\nu_{20}$ (B_1) (857)	861.1 w	862.0	16.4	459.1	
$\nu_{27}-\nu_{11}$ (B_2) (845)		846.8	11.6	88.0	
ν_{13} (A_2)	830.7 w	832.4	11.5	843.4	
$\nu_{24}-\nu_{29}$ (A_1) (830); $\nu_{28}-\nu_{30}$ (A_1) (823)		826.2	10.0	383.9	
$\nu_9-\nu_{20}$ (B_1) (815)	810.8 w	809.9	11.6	327.9	
$\nu_5-\nu_{17}$ (B_1) (738); $\nu_{23}-\nu_{13}$ (B_1) (737)	739.7	739.9	5.2	14511.7	68645.4
ν_{17} (B_1)	735.3 s	736.0	4.9	31371.9	
		733.0	4.8	22761.8	
	691 tail m	690.8	4.0	737.2	20260.6
ν_{18} (B_1)	683.7 s	683.9	4.5	19523.4	
$\nu_{15}-\nu_{11}$ (B_1) (674); $\nu_4-\nu_{16}$ (B_1) (676)		673.2	2.6	2852.2	13539.6
ν_{10} (A_1)	672.4 s	672.0	3.0	7671.8	
	669 sh s	669.0	4.6	1878.8	
$\nu_{28}-\nu_{14}$ (B_1) (661);	662 tail m	662.3	7.6	1136.8	
$2\nu_{11}$ (A_1) (625)	627.0 w	626.5	11.7	665.0	
ν_{29} (B_2)	612.2 m	612.4	2.6	350.8	
$\nu_{23}-\nu_{12}$ (B_1) (608); $\nu_{24}-\nu_{13}$ (B_1) (610); $\nu_7-\nu_{19}$ (B_1) (610)	607 tail w	I			
$\nu_{14}+\nu_{20}$ (B_2) (594)	596.0 w	I			
$\nu_{11}+\nu_{30}$ (B_2) (559); $\nu_8-\nu_{19}$ (B_1) (562); $\nu_6-\nu_{29}$ (B_2) (561); $\nu_4-\nu_8$ (A_1) (559)	558.8 w	557.4	7.6	39.4	
$\nu_9-\nu_{19}$ (B_1) (542)	541.7 w	541.7	4.5	46.8	
ν_{19} (B_1)	457.3 s	457.6	3.7	8110.3	9570.8
$\nu_{28}-\nu_{29}$ (A_1) (457); $\nu_5-\nu_8$ (A_1) (455)	tail s	455.9	3.7	1460.5	
ν_{11} (A_1)	312.8 m	312.7	10.2	1299.3	
$\nu_{24}-\nu_{27}$ (A_1) (285); $\nu_8-\nu_{17}$ (B_1) (283)	288.1 vw	I			
ν_{30} (B_2)	246.6 w	246.3	6.2	17.8	
$\nu_5-\nu_{26}$ (B_2) (211); $\nu_{29}-\nu_{14}$ (B_1) (203)	206.4 w	I			
ν_{20} (B_1)		184.7	13.1	420.2	852.6
$\nu_{24}-\nu_{26}$ (A_1) (179)	179.3 m	178.7	8.7	279.6	
$\nu_6-\nu_9$ (A_1) (174)		172.9	8.6	152.8	

[a] Herzberg's notation is used to number the vibrations. The assignments are limited to fundamentals, first overtones and active binary sum and difference bands. WV − indicates that the band is assigned to water vapor. [b] The unit is cm^{-1}. S indicates strong, m medium, w weak, vw very weak, sh shoulder, br broad. [c] The unit is cm^{-1}. I indicates weak feature ignored in the fit. [d] The unit is cm mol^{-1}. Divide the values by 1×10^5 to get value in the usual unit of km mol^{-1}.

point group C_{2v}, where by convention the *x*-axis is taken orthogonal to the plane of the molecule. Herzberg's notation[15] is used to number the vibrations throughout this paper. The A_2 vibrations are infrared inactive in the gas phase and the others are infrared active. All first overtones and binary sum and difference bands except $A_1 \times A_2$ and $B_1 \times B_2$ are infrared active.

Included in Table 1 are the assignments of most of the bands used to fit the spectrum. The fundamentals, including the infrared inactive fundamentals that may be activated in the liquid phase, were assigned with the aid of the literature assignments of bromobenzene,[16,17] chlorobenzene,[18] and benzene-*d*[19] as well as the liquid phase force field of benzene.[20] The liquid force field of benzene was used with the **G** matrix calculated for bromobenzene to calculate the wavenumbers of the fundamentals. The C−Br bond length of 1.865 Å given by Radcliffe and Steele,[21] the C−C and C−H bond lengths of 1.3920 and 1.0862 Å, respectively, determined by Plíva et al.,[22] and the carbon-12

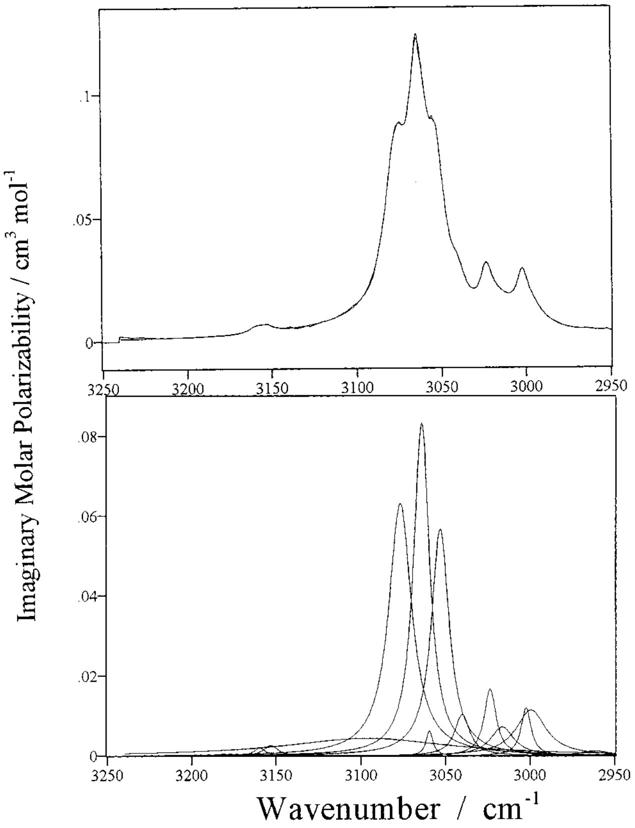

Figure 6. The experimental and fitted imaginary molar polarizability spectra (top box) of liquid C_6H_5Br at 25 °C between 3240 and 2950 cm^{-1} and the CDHO bands used to achieve the fit (bottom box).

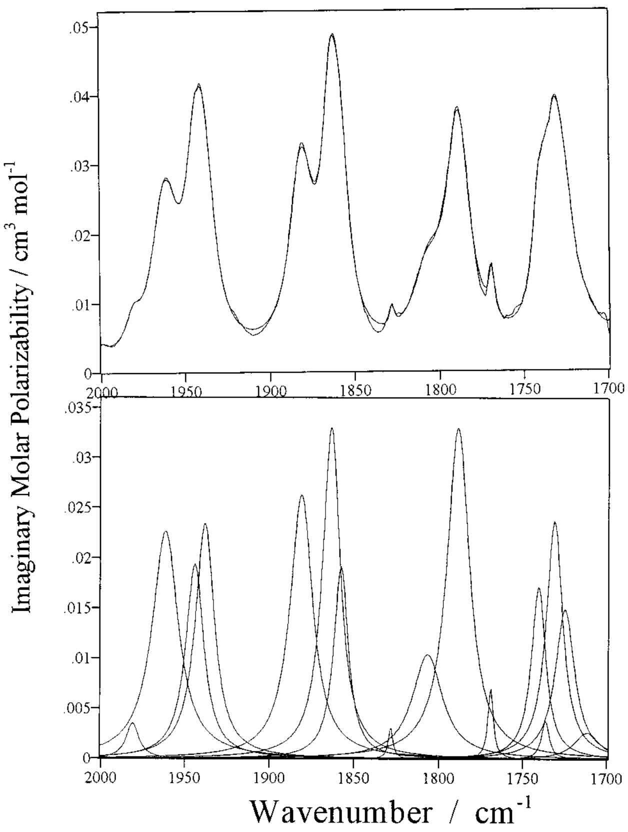

Figure 7. The fitted and experimental imaginary molar polarizability spectra (top box) of liquid C_6H_5Br at 25 °C between 2000 and 1700 cm^{-1} and the CDHO bands used to achieve the fit (bottom box).

atomic mass scale masses of 79.904, 12.000, and 1.007825 u were used to calculate the **G** matrix. This takes into account the changes in mass but it does not account for any differences in the force fields of benzene and bromobenzene. These calculated wavenumbers are therefore not expected to match the experimental wavenumbers for vibrations that involved the bromine but they should predict the CH stretching wavenumbers very well, at least the order of the A_1 and B_2 vibrations. The calculated and experimental wavenumbers of the fundamentals are given in Table 2. Most of the calculated wavenumbers agree with the experimental wavenumbers to within 10 cm^{-1}. These calculated wavenumbers were used only to determine the pattern for the CH stretching vibrations. The calculated order was ν_{21}, ν_1, ν_2, ν_3, and ν_{22}, the same as for C_6H_5D,[19] thus the CH stretches were confidently assigned with this pattern.

The assignments of the remaining bands are limited to first overtones and active binary sum and difference bands because ternary and larger combinations allow too many possibilities. It is expected that the first overtones and binary sum and difference bands should be the most intense, but it is noted that other overtones and combinations are possible and it is an impossible task to assign them from the current experimental measurements. The assignments are presented as most probable assignments, and when the experimental work is complete on the monosubstituted benzenes (C_6H_5D, C_6H_5F, C_6H_5Cl, C_6D_5F, C_6D_5Br, C_6D_5Cl) some refinement of these assignments may be possible. The assignments were kept as close to the assignment of C_6H_5D [19] as possible. Since the value of ν_{14} was not determined in this work, it was taken to be at 409 cm^{-1}, as given in ref 16, to calculate the wavenumbers of the sum and difference bands.

Transition Moments of Fundamentals. Under the assumption that all of the hot bands of the fundamental contribute to the fundamental band, the dipole transition moment, R_j, is related to the integrated intensity, C_j through eq 2 [3,23-25]

$$|\boldsymbol{R}_j| = \sqrt{\frac{3hc_0}{N_A \pi g_j \tilde{\nu}_j} C_j} \qquad (2)$$

Under the assumption of mechanical and electrical harmonicity, the square of the dipole moment derivative with respect to the jth normal coordinate, μ_j^2, can be obtained from C_j through eq 3[3]

$$\mu_j^2 = \frac{24\pi c_0^{\,2}}{N_A g_j} C_j \qquad (3)$$

where in eqs 2 and 3, N_A is Avogadro's number, h is Planck's constant, c_0 is the velocity of light in a vacuum, and g_j is the degeneracy of the jth vibration.

The transition moment, $\boldsymbol{R}_j$, and the square of the dipole moment derivative with respect to the normal coordinate, μ_j^2, were calculated for each of the fundamentals via eqs 2 and 3, respectively. These values are presented in Table 3. Also included in Table 3 are the literature[19] transition moments, $\boldsymbol{R}_j$, and the squares of the dipole moment derivatives with respect to the normal coordinates, μ_j^2, for the fundamentals of benzene-*d*. It is obvious from Table 3 that the transition moments and dipole moments are significantly different between bromobenzene and benzene-*d*.

It is tempting to attribute this difference in transition moments and dipole moment derivatives with respect to normal coordinates to changes in the dipole moment derivatives with respect to symmetry and internal coordinates. However, differences in

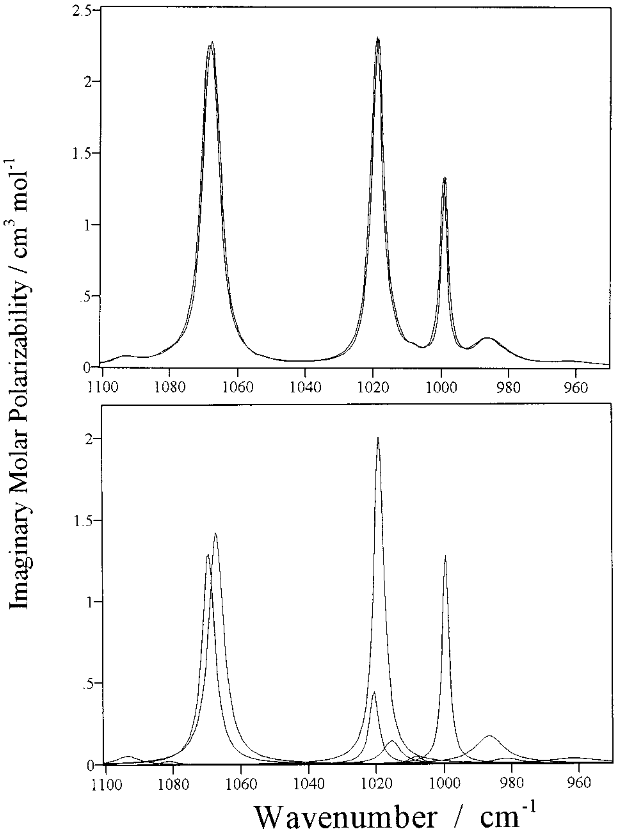

Figure 8. The fitted and experimental imaginary molar polarizability spectra (top box) of liquid C_6H_5Br at 25 °C between 1100 and 950 cm^{-1} and the CDHO bands used to achieve the fit (bottom box).

the experimental observed dipole moment derivatives can be due to a change in the eigenvectors without a change in the dipole moment derivatives with respect to symmetry and internal coordinates. To determine if the differences between bromobenzene and benzene-*d* are due to changes in the dipole moment derivatives with respect to the symmetry and internal coordinates or changes in the eigenvectors, it is necessary to obtain the dipole moment derivatives with respect to symmetry or internal coordinates. This requires the eigenvectors of an accurate liquid force field calculation for bromobenzene. In order to have enough information to obtain these eigenvectors, the optical constants of bromobenzene-d_5 must be obtained.

Extensions. Work is currently under way in this laboratory to measure the optical constants of bromobenzene-d_5. Once these optical constants have been measured and the imaginary molar polarizability spectrum fitted, it will be possible to use the combined bromobenzene and brombenzene-d_5 intensities and wavenumbers to calculate the liquid phase force field and eigenvectors. The intensities can then be related to the dipole moment derivatives with respect to the symmetry and internal coordinates and thus facilitate a more complete comparison among the monosubstituted benzenes.

Summary

The first detailed vibrational assignment of liquid bromobenzene is reported. The imaginary molar polarizability spectrum, $\alpha''_m(\tilde{\nu})$, was fitted with 163 CDHO bands and the integrated intensity, C_j, calculated analytically from the fitted parameters for each band. The transition moments and squares of the dipole moment derivatives with respect to normal coordinates were calculated for bromobenzene and compared with those reported elsewhere[19] for benzene-*d*. From this comparison, it is obvious that the transition moments and dipole moment derivatives with respect to normal coordinates are different in these two

TABLE 2: Calculated and Experimental Wavenumbers of Fundamentals of Bromobenzene

		wavenumber/cm^{-1}		
vibration	symmetry	calcd harmonic[a]	calcd anharmonic[a]	exptl
ν_1	A_1	3180	3063	3064.4
ν_2	A_1	3167	3050	3053.4
ν_3	A_1	3158	3041	3040.3
ν_4	A_1	1586	1580	1578.4
ν_5	A_1	1472	1462	1474.1
ν_6	A_1	1273	1273	1173.6
ν_7	A_1	1152	1152	1067.2
ν_8	A_1	1013	1013	1019.1
ν_9	A_1	1000	998	999.6
ν_{10}	A_1	745	745	672.0
ν_{11}	A_1	305	305	312.7
ν_{12}	A_2	973	973	961.6
ν_{13}	A_2	853	853	832.4
ν_{14}	A_2	403	403	409[16]
ν_{15}	B_1	984	984	986.7
ν_{16}	B_1	913	913	902.4
ν_{17}	B_1	735	735	736.0
ν_{18}	B_1	698	698	683.9
ν_{19}	B_1	451	451	457.6
ν_{20}	B_1	167	167	184.7
ν_{21}	B_2	3187	3070	3076.9
ν_{22}	B_2	3151	3034	3023.8
ν_{23}	B_2	1560	1560	1569.6
ν_{24}	B_2	1423	1423	1442.6
ν_{25}	B_2	1327	1327	1321.0
ν_{26}	B_2	1276	1276	1263.4
ν_{27}	B_2	1152	1152	1157.4
ν_{28}	B_2	1052	1052	1069.5
ν_{29}	B_2	580	580	612.4
ν_{30}	B_2	205	205	246.3

[a] Calculated using the liquid benzene force field of ref 20. The anharmonic corrections of Goodman et al. (Goodman, L; Ozkabak, A. G.; Thakur, S. N.; *J. Phys. Chem.* **1991**, *95*, 9044) were used in ref 20 and this work.

TABLE 3: Transition Moments and Square of the Dipole Moment Derivatives with Respect to Normal Coordinates of Fundamentals of Bromobenzene and Benzene-*d*

	C_6H_5Br			C_6H_5D (ref 19)		
	$\tilde{\nu}_j$/cm^{-1}	$\lvert\boldsymbol{R}_j\rvert$/D	μ_j^2/(D^2 Å^{-2} u^{-1})	$\tilde{\nu}_j$/cm^{-1}	$\lvert\boldsymbol{R}_j\rvert$/D	μ_j^2/(D^2 Å^{-2} u^{-1})
ν_1	3064.4	0.0217	0.0854	3064.3	0.0344	0.215
ν_2	3053.4	0.0190	0.0652	3060	not observed	
ν_3	3040.3	0.00744	0.00999	~3052	0.0149	0.0400
ν_4	1578.4	0.0508	0.242	2269.0	0.0266	0.0953
ν_5	1474.1	0.0743	0.482	1592.6	0.0116	0.0126
ν_6	1173.6	0.0201	0.0281	1475.2	0.0439	0.168
ν_7	1067.2	0.0613	0.238	1175.3	0.0158	0.0175
ν_8	1019.1	0.0604	0.221	1032.3	0.0431	0.114
ν_9	996.3	0.0391	0.0906	1007.1	0.0131	0.0103
ν_{10}	672.0	0.0798	0.253	981.6	0.0133	0.0103
ν_{11}	312.7	0.0362	0.0243	~602	not observed	
ν_{12}	961.6	0.0166	0.0157	not observed		
ν_{13}	832.4	0.0179	0.0158	not observed		
ν_{14}	not measured			not observed		
ν_{15}	986.7	0.0296	0.0514	~988	0.0140	0.0115
ν_{16}	902.4	0.0350	0.0656	925.6	0.0304	0.0506
ν_{17}	736.0	0.171	1.28	779.6	0.0983	0.447
ν_{18}	683.9	0.0966	0.379	698.7	0.0896	0.333
ν_{19}	457.6	0.0812	0.179	607.3	0.176	1.12
ν_{20}	184.7	0.0381	0.0159	~380	not observed	
ν_{21}	3076.9	0.0277	0.140	3079.8	0.0356	0.232
ν_{22}	3023.8	0.00837	0.0126	3032.9	0.0121	0.0263
ν_{23}	1569.6	0.0342	0.109	1575.2	0.0103	0.0100
ν_{24}	1442.6	0.0496	0.211	1449.9	0.0445	0.171
ν_{25}	1321.0	0.0192	0.0288	1316.7	0.0061	0.0030
ν_{26}	1263.4	0.0179	0.0240	1297.6	0.0080	0.0050
ν_{27}	1157.4	0.0189	0.0245	1158.4	0.0194	0.0260
ν_{28}	1069.5	0.0537	0.183	1076.1	0.0295	0.055
ν_{29}	612.4	0.0134	0.00656	857.7	0.0387	0.0762
ν_{30}	246.3	0.00477	0.00033	601.8	not observed	

molecules. To determine if these differences are due to changes in the dipole moment derivatives with respect to the internal coordinates or if they are due completely to changes in eigenvectors, the optical constants of bromobenzene-d_5 are going to be measured and a more complete analysis will be presented in a future paper.

Acknowledgment. C.D.K. thanks the Natural Sciences and Engineering Research Council of Canada and the Research Evaluation Committee of the University College of Cape Breton for research grants in support of this work. C.D.K. and S.D.F. thank the Students Works program for their support of this work.

References and Notes

(1) Keefe, C. D.; Pittman, J. *Appl. Spectrosc.* **1998**, *52*, 1062.

(2) Fleming, J. W.; Turner, P. A.; Chantry, G. W. *Mol. Phys.* **1970**, *19*, 853.

(3) Bertie, J. E.; Zhang, S. L.; Keefe, C. D. *J. Mol. Struct.* **1994**, *324*, 157.

(4) Bertie, J. E.; Keefe, C. D.; Jones, R. N. *Can. J. Chem.* **1991**, *69*, 1609.

(5) Bertie, J. E.; Zhang, S. L.; Keefe, C. D. *Vib.Spectroc.* **1995**, *8*, 215.

(6) Goplen, T. G.; Cameron, D. G.; Jones, R. N. *Appl. Spectrosc.* **1980**, *34*, 657.

(7) Timmermans, J. *Physico-chemical constants of pure organic compounds.* Elsevier: New York, 1950; pp 287−289.

(8) Bertie, J. E.; Zhang, S. L. *Can. J. Chem.* **1992**, *70*, 520.

(9) Bertie, J. E.; Jones R. N.; Keefe, C. D. *Appl. Spectrosc.* **1993**, *47*, 891.

(10) Bertie, J. E.; Jones, R. N.; Apelblat, Y.; Keefe, C. D. *Appl. Spectrosc.* **1994**, *48*, 127.

(11) Bertie, J. E.; Jones, R. N.; Apelblat, Y. *Appl. Spectrosc.* **1994**, *48*, 144.

(12) Bertie, J. E.; Lan, Z.; Jones, R. N.; Apelblat, Y. *Appl. Spectrosc.* **1995**, *49*, 840.

(13) Bertie, J. E.; Keefe, C. D. *Fresenius J. Anal. Chem.* **1998**, *362*, 91. YACFIT5 is the YACFIT program described in ref 13, with the array sizes increased to allow up to 400 peaks and compiled using Digital Fortran 5.0 to operate under Microsoft Windows NT. YACFIT5 is available from Prof. John Bertie, Department of Chemistry, University of Alberta, Edmonton, Alberta, T6G 2G2.

(14) McClave, J. T.; Dietrich, F. H., II; Sincich, T. *Statistics*, 7th ed.; Prentice Hall: Upper Saddle River, 1997; Chapter 12.

(15) Herzberg, G. *Molecular Spectra and Molecular Structure. II. Infrared and Raman Spectra of Polyatomic Molecules*; D. Van Nostrand Company, Inc.: Princeton, 1945.

(16) Varsányi, G. *Assignments for Vibrational Spectra of Seven Hundred Benzene Derivatives*; John Wiley & Sons: New York, 1974; Vol. 1.

(17) Roeges, N. P. G. *A Guide to the Complete Interpretation of Infrared Spectra of Organic Structures*; John Wiley & Sons: Chichester, 1994.

(18) Bertie, J. E.; Apelblat, Y., in preparation.

(19) Bertie, J. E.; Keefe, C. D.; Apelblat, Y., submitted to *J. Mol. Struct.*

(20) Keefe, C. D. *Absolute Infrared Absorption Intensities of Liquid Benzene*, Ph.D. Thesis, University of Alberta, Edmonton, 1994.

(21) Radcliffe, K.; Steele, D. *Spectrochim. Acta* **1969**, *25A*, 597.

(22) Plíva, J.; Johns, J. W. C.; Goodman, L. *J. Mol. Spectrosc.* **1991**, *148*, 427.

(23) Fahrenfort, J. In *Infra-red Spectroscopy and Molecular Structure*; Davies, M., Ed.; Elsevier: Amsterdam, 1963.

(24) Warner, J. W.; Wolfsberg, M. *J. Chem. Phys.* **1983**, *78*, 1722.

(25) Dignam, M. J. *Appl. Spectrosc. Rev.* **1988**, *24*, 99.